Carbohydrate Polymers 114 (2014) 27–35

Contents lists available at ScienceDirect

Carbohydrate Polymers

journal homepage: www.elsevier.com/locate/carbpol

Oxidation and pH responsive nanoparticles based on ferrocene-modified chitosan oligosaccharide for 5-fluorouracil delivery

Youqian Xu, Liang Wang, Ya-Kun Li, Cai-Qi Wang*

School of Chemistry and Chemical Engineering, University of Chinese Academy of Sciences, Beijing 100049, China

ARTICLE INFO

Article history:
Received 15 May 2014
Received in revised form 31 July 2014
Accepted 1 August 2014
Available online 10 August 2014

Keywords:
Ferrocene
Chitosan oligosaccharide
Stimuli-responsive nanoparticles
5-Fluorouracil
Synergistic effect

Chemical compounds studied in this article:
5-Fluorouracil (PubChem CID: 3385)
Sodium hypochlorite (PubChem CID: 23665760)
Hydrogen peroxide (PubChem CID: 784)
Sodium tetrahydridoborate (PubChem CID: 4311764)
Ferrocenecarboxaldehyde (PubChem CID: 114595)

ABSTRACT

Stimuli-responsive nanoparticles based on biodegradable and biocompatible saccharides are potentially superior carriers under different physical conditions. In this study, we present a detailed investigation on the oxidation and pH responses of ferrocene-modified chitosan oligosaccharide (FcCOS) nanoparticles for 5-Fluorouracil (5-FU) Delivery. The dispersion of FcCOS nanoparticles depends strongly on pH change. NaClO, H_2O_2 and oxygen, as oxidant models, in a weak acid solution displayed varying accelerations as the disassembly progressed. 5-FU, as a drug model, is efficiently uploaded in FcCOS nanoparticle (approximately 238 nm). The in vitro release of 5-FU from FcCOS nanoparticles studies show that the accumulative release increased with the decrease of pH under bubbled N_2. Interestingly, the sample under bubbled air has a higher accumulative release up to 59.64% at pH 3.8, compared with samples under bubbled N_2 just 49.02%. The results suggested that FcCOS nanoparticles disassembled faster and the release of drug molecules was accelerated because of the synergistic effect of oxidative agent and low pH. Thus, FcCOS can be developed as an effective pH and oxidation dual-responsive carrier to enhance drug efficacy for cancer treatment.

1. Introduction

Nanoparticles that are sensitive to redox potential, pH and temperature have attracted considerable attention in nanomedicine because their structures can be altered by small external changes (Angelatos, Radt, & Caruso, 2005; Chen et al., 2014; Cheng, Meng, Deng, Klok, & Zhong, 2013; Li & Keller, 2009; Motornov, Roiter, Tokarev, & Minko, 2010; Zhou, Du, Cui, & Zhang, 2013). In contrast to a single-stimulus system, a dual-stimuli system shows a synergistic effect, thereby enhancing the recognition efficiency for targeting tumors. Dual-stimuli responsive nanoparticles have shown distinct drug delivery and release behaviors, leading to superior anti-cancer efficacy (Kumar & De, 2014; Xuan, Han, Xia, & Zhao, 2014). The dual stimuli, redox potential and pH, have attracted attention because activities of oxidative and pH microenvironments are different between tumor and healthy cells in vivo (Ge & Liu, 2013). The pH of tumor internal environment is lower than that of normal physiological environment, which is advantageous in designing pH-responsive drug carriages. At the same time, reactive oxygen species (ROS) and other oxidants have important functions in several physiological processes, such as cell signaling and metabolism (Borrelli et al., 2014; Song, Ji, Du, & Li, 2013). Thus, nanocarriers that are responsive to the described bio-relevant stimuli or characteristic biochemical signals in pathologic tissues and cells may be utilized to enhance therapeutic efficacy.

Although much progress has been made on the assembly of nanoparticles stimulated by pH and oxidation, challenges for clinical application still exist (Ge & Liu, 2013). Nanoparticles designed for biomedical applications should be biocompatible, biodegradable, and non-toxic. However, currently available constructed nanocarriers are mainly based on organic/inorganic hybrid or blocked part biocompatible and biodegradable materials (Ge &

* Corresponding author at: School of Chemistry and Chemical Engineering, University of Chinese Academy of Sciences, 19A Yuquan Road, Beijing 100049, PR China. Tel.: +86 10 88256920; fax: +86 10 88256093.
E-mail addresses: wang-caiqi@ucas.ac.cn, wang.caiqi@sohu.com (C.-Q. Wang).

http://dx.doi.org/10.1016/j.carbpol.2014.08.003
0144-8617/

Liu, 2013; Salonen et al., 2005; Wang, Chen, Ding, & Yan, 2012; Xuan et al., 2014). Chitosan oligosaccharide (COS), the oligomer of chitosan (CS), has been utilized to fabricate amphiphilic biofunctional materials because COS possesses excellent biocompatibility, biodegradability, and desirable bioactivity for biological applications (Kim & Rajapakse, 2005; Xia, Liu, Zhang, & Chen, 2011). COS can also inhibit the growth of tumor cells by exerting immune enhancing effects via increased production of lymphokines (Xia et al., 2011). Thus, COS has attracted considerable interest in the preparation of drug or gene carriers for drug delivery applications. The responsive assembly of COS derivatives to temperature and pH have been investigated (Shi, Alves, & Mano, 2008; Sun, Shi, Xu, & Cao, 2013; Wei, Luo, Fu, Zhang, & Ma, 2012). However, the response of COS derivatives to oxidation receives relatively less attention.

Ferrocene (Fc) is an organometallic compound that consists of two cyclopentadienyl (Cp) rings bound on the opposite sides of a central metal atom, which is known for its redox properties and hydropobicity (Duan et al., 2013; Liu et al., 2012; Zhu, Shangguan, Sun, Ji, & Zheng, 2010). The interconversion between Fe(II) and Fe(III) states results in the hydrophobicity to hydrophilicity transition of the hydrophobic block of Fc-containing amphiphiles (Zhu et al., 2010). Therefore, Fc is exploited in designing stimuli-sensitive assemblies, which acted as both hydrophobic moiety and redox-responsive trigger (Fouda, Abd-Elzaher, Abdelsamaia, & Labib, 2007; Top et al., 2001). Many ferrocenyl derivatives have excellent effects as antitumor agents, and some derivatives are now in clinical trials (Fouda et al., 2007; Top et al., 2001). Therefore, Fc derivative assembly equipped with pH responsive characteristics has a unique advantage in the drug delivery system.

5-Fluorouracil (5-FU), a pyramidine analogue that interferes with thymidylate synthesis, has been employed extensively in clinical chemotherapy for the treatment of solid tumors (Wen, Li, & Wu, 2012). However, the use of 5-FU is still limited by its rapid metabolism, short biological half-life, non-uniform absorption, and nonselective action against healthy cells (Rejinold, Muthunarayanan, Chennazhi, Nair, & Jayakumar, 2011). CS is useful for the prevention of side effects, such as myelotoxicity, gastrointestinal toxicity, and immunotoxicity that are caused by 5-FU (Aydin & Pulat, 2012; Kimura & Okuda, 1999; Yang & Hon, 2009). Given these properties, COS can be the most suitable candidate for 5-FU delivery.

Recently, our group presented a novel and facile method for constructing micro-size "snowflake-like" assemblies that respond to pH and oxidation stimuli. The "snowflake-like" assemblies with micron size are formed via the self-organization of Fc-modified COS with substitution degree as 0.24 in an acid aqueous solution (Wang, Li, Xu, & Wang, 2014). However, the controlled release behavior of drug-load FcCOS assemblies under various pH buffers and bubbled oxygen was not concerned. In this work, oxidation and pH responsive nanoparticles based on FcCOS for 5-FU Delivery were detailedly investigated. 5-FU was loaded in FcCOS nanoparticles and the controlled release behavior under various pH buffers and bubbled oxygen in weak acid solutions was evaluated.

2. Experimental

2.1. Materials

Chitosan oligosaccharide (COS) (M_W < 3000, deacetylation degree 92%) was purchased from Dalian GlycoBio Co. Ltd. Ferrocene carboxaldehyde (FcCHO) (98%) and 5-fluorouracil (5-Fu) (99%) were obtained from J&K Chemical Ltd. Sodium hypochlorite (NaClO) (≥8.0%, analytical grade) was purchased from Xilong Chemical Co. Ltd. Hydrogen peroxide (H_2O_2) (≥30%, analytical grade) was obtained from Beijing Chemical Works. Sodium borohydride ($NaBH_4$) was purchased from Sinopharm Chemical Reagent Co. Ltd. All the other chemical reagents in the study were in analytical grade and utilized without further purification. Deionized water (specific resistance 18.25 MΩ) was used in all experiments.

2.2. Synthesis of Fc-modified COS

Fc-modified COS (FcCOS) was synthesized according to the previous literature (Garcia, Peniche-Covas, Chico, Simpson, & Villalonga, 2007). COS (1.93 g, 11 mmol -NH_2) was dissolved in 20 mL of aqueous acetic acid (3.0 wt%) and FcCHO (2.57 g, 12.01 mmol) solution in 20 mL methanol was added dropwise under the protection of nitrogen (N_2). The mixed solution was vigorously stirred at room temperature for 1 h, and $NaBH_4$ (1.36 g, 36 mmol) was added and left stirred for 4 h. 5.0% NaOH aqueous solution was instilled to quench the reaction until the pH of the system reached 10. The resulting yellowish-brown precipitate was detached by centrifugation and washed with 90% methanol repeatedly until the absence of FcCHO was confirmed by spectrophotometer in the elution. The solid products were dried under vacuum at ambient temperature.

2.3. The degree of substitution of ferrocene

The degree of substitution of ferrocene (DS_{Fc}) on COS was quantified by UV–vis spectrophotometer according to following equation:

$$DS_{Fc} = \frac{c_{Fc}V/M_{Fc}}{DD \times \left[m - (M_{Fc} - 16)(c_{Fc}V/M_{Fc})\right]/M_{avg}} = \frac{c_{Fc}M_{Fc}}{DD \times (c_0 M_{Fc} - c_{Fc}M_{Fc} + 16c_{Fc})} \quad (1)$$

where c_{Fc} is the ferrocene concentration of resultant determined by UV–vis spectrophotometer, mg/mL; DD is the deacetylation degree of COS; M_{avg} is the average molecular weight of COS unit, mg/mL; V is the volume of the sample, mL; c_0 is the concentration of the sample, mg/mL; M_{Fc} is the molecular weight of FcCHO, mg/mmol; 16 is the difference in molecular weight before and after modification.

2.4. Preparation of FcCOS nanoparticles

The nanoparticles of FcCOS were prepared in the acid aqueous solution of HAc (2 wt%), followed by sonication for 30 min (KQ-50B ultrasonic bath, Kunshan Ultrasonic Instrument Co., China, 50 W). The morphology and size distribution of the nanoparticles were tested by TEM and DLS respectively.

2.5. Determination of critical nanoparticle concentration (CMC)

The critical micelle concentration (CMC) was determined by surface tension. Contact angle of 5 μL water droplet on the tetrafluoroethylene platform was measured with intravenous drip contact angle instrument (JC2000C1, Shanghai Zhongchen Digital Technology Co., Ltd.) at 25 °C and repeated at least three times.

2.6. pH responses of the FcCOS nanoparticles

The nanoparticles solution was prepared with the concentration of 1 mg/mL. The pH of the solution was adjusted by HAc and NaOH to investigate the change of FcCOS nanoparticles. The performance at different pH values were determined by UV–vis spectrophotometer.

2.7. Oxidation responses of FcCOS nanoparticles

FcCOS nanoparticles freshly prepared were tested by UV–vis spectrophotometer under different conditions. NaClO, H_2O_2 and air were utilized to confirm the oxidation response. Various quantities of H_2O_2 and NaClO were added into 1.0 mL freshly prepared nanoparticle solution at 1.0 mg/mL, and they were checked by UV–vis after 5 min. The test sample solution at pH 3.8 was bubbled with air and measured by UV–vis at predetermined time points.

2.8. Preparation of 5-FU-loaded FcCOS nanoparticles

5-FU was dissolved in ethanol by ultrasonic dispersion method and solvent was removed under vacuum drying at 25 °C for 4 h. Then FcCOS dissolved in HAc (2 wt%) aqueous was added. The proportion of drugs was kept as 15.86%. The sample was treated with ultrasound and then was freeze-dried to remove moisture. Finally, the product was washed three times with absolute ethanol to remove the unentrapped 5-FU and then dried under vacuum.

2.9. Estimation of drug loading and encapsulation efficiency

Loading efficiency of 5-FU in nanoparticles was determined by UV–vis spectrophotometer. 1.1 mg of drug-load nanoparticles were ultrasonically dispersed in 10 mL ethanol. Keeping standing for 5 h, the resultant solution was filtered and tested by UV–vis spectrophotometer. The loading capacity and encapsulation efficiency were calculated according to Eqs. (2) and (3), respectively.

$$\%\text{Loading Capacity} = \left(\frac{\text{amount of drug in beads}}{\text{amount of initial drug}}\right) \times 100 \quad (2)$$

$$\%\text{Encapsulation Efficiency} = \left(\frac{\text{actual loading}}{\text{theoretical loading}}\right) \times 100 \quad (3)$$

2.10. In vitro 5-FU release from 5-FU/FcCOS nanoparticles

Phosphate-buffered saline (PBS) and acetic acid-sodium acetate (HAc-NaAc), at different pH values, were used as the dissolution medium for the 5-FU release tests. 1.5 mL 5-FU/FcCOS was added into a dialysis bag (MWCO: 3.5 kDa, Solarbio) and then transferred into a glass vessel containing 20 mL buffers. The vessels were placed in an incubator shaker (SPH-110A, SHIPING) maintaining at 37 °C and shaken whirly at 200 rmp. At predetermined time intervals, 3 mL medium of the dialysis bag was withdrawn, and then 3 mL fresh buffers was added into the primary system. The drug concentration was determined by UV–vis spectrophotometer at 266 nm.

2.11. Characterization

The chemical structure of FcCOS was confirmed through Fourier transform infrared spectroscopy (FT-IR) (AVATAR 360, Thermo-Nicolet). The samples for FT-IR analysis were prepared by dispersing the powder of FcCOS in KBr and compressing the mixtures with model to form disks, and tested in the range of 400–4000 cm^{-1}. X-ray diffraction (XRD) analysis of sample was recorded from 5° to 35° with a X-ray powder diffractometer (MSAL XD-2) which worked with CuKα irradiation (λ = 0.15406 nm, 36 kV, 18 mA). ^{1}H NMR spectra were recorded on a JEOL JNM-ECA600 spectrometer operating at 600 MHz using 2% trifluoroacetic acid/deuterium oxide (v/v) as a solvent. The chemical shifts were calibrated against residual solvent signals of HOD. UV–vis spectra were recorded by a UV–vis spectrometer (Shimadzu UV-2500) using a cuvette with a light path length of 1.0 cm. Dynamic light scattering (DLS) measurements at 25 °C were performed using a NICOMP380 ZLS Particle Sizer equipped with a 5.0 mW laser operating at λ = 633 nm with a scattering angle of 90°. Cyclic voltammetry (CV) measurements were performed with an electrochemical workstation (CHI660C, Shanghai Chenhua Equipments, China). The electrochemical cell at the ambient temperature consisted of a three-electrode system with a GCE (0.071 cm^2) as the working electrode, a platinum wire as the counter electrode, and a saturated calomel electrode (SCE) as the reference electrode. All potentials were referenced to the SCE. To obtain pure working solution without oxygen, nitrogen would be bubbled into the solution within whole process. Scan rate was kept as 0.1 V/s. The images of the nanoparticles were obtained at ambient temperature using a TECNAI T20 transmission electron microscope (TEM). Tested samples for TEM observation were prepared by dropping the certain solution onto carbon-coated copper grid and dried at ambient temperature. And all samples need no further staining.

3. Results and discussion

3.1. Synthesis and characterization of FcCOS

The synthesis products were analyzed by FT-IR and ^{1}H NMR. In the FT-IR spectra of FcCOS, the new absorption band appears at 490 cm^{-1} is assigned to the M-ring stretch and ring tilt of Fc. Compared with the original COS, the relative intensity of the absorption band at 1645 cm^{-1} versus 1558 cm^{-1} is attributed to the consumption of the amino group (Fig. 1A). In the ^{1}H NMR spectrum shown in Fig. 1B, the structure of FcCOS was determined from the new peak attributed to the protons of the Cp rings in the range of 4.0 ppm to 4.4 ppm, indicating the successful synthesis of the amphiphile FcCOS. However, given the overlap with the solvent (HOD), estimating the amount of ferrocenyl groups connected to the COS backbone from the ratio of integral signals is impossible (Hirai, Odani, & Nakajima, 1991).

The DS_{Fc} was quantified by the UV–vis spectrophotometer. As shown in Fig. 1C, the characteristic absorption band of Fc detected at approximately 472 nm in the FcCOS spectrum in a mixed solvent that consists of 1.0% (v/v) AcOH aqueous solution and methanol at a volume ratio of 1:1. Quantified by UV–vis spectrophotometry, the DS_{Fc} is 0.40, which means that the Fc group that would respond to oxidation stimuli is grafted efficiently and that a major part of amino groups would respond to pH variations.

The crystalline ability of FcCOS in solid state was determined by XRD (Fig. 1D). The broad peaks around 2θ = 20–21° of COS and FcCOS shows that the COS backbone structure is amorphous. Meanwhile, the wide peak around 14.8° in the profile of FcCOS can be attributed to the π–π stacking of the Fc group. Therefore, the structure of Fc grafted onto COS improved the crystalline ability in bulk compared with the original materials, which can be beneficial to form well-organized assemblies with special morphologies in the solution (Clark & Smith, 1936). The stable structure is expected to have excellent drug delivery performance.

3.2. Self-assembly research of FcCOS

CMC is an important parameter to estimate the micellization ability of amphiphilic molecules. Surface tension, a commonly used indicator to measure CMC (Weschayanwiwat, Scamehorn, & Reilly, 2005), changes from micellar to true solution. As shown in Fig. 1E, the CMC of FcCOS was approximately 0.042 mg/mL in 1.0 wt% AcOH aqueous solution.

The self-assembled behavior of FcCOS in acid solution (1.0 wt% AcOH) was investigated. The irregular spherical particles at different concentrations were observed by TEM, and the average size of

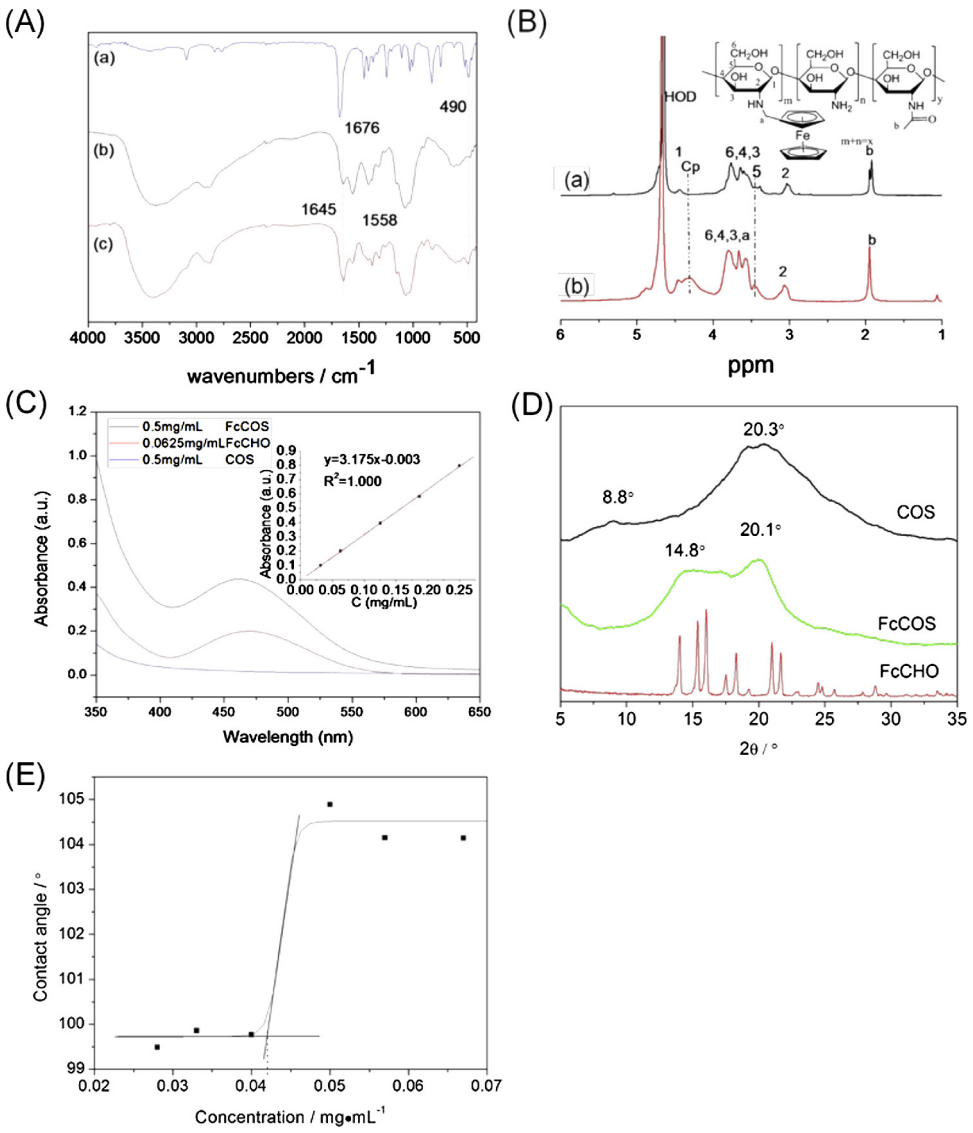

Fig. 1. (A) FT-IR spectrum of (a) original FcCHO; (b) original COS and (c) FcCOS samples; (B) ^{1}H NMR of (a) COS and (b) FcCOS; (C) UV–vis of FcCOS, FcCHO and COS: FcCOS (0.5 mg/mL); COS (0.5 mg/mL); (D) XRD of COS, FcCOS and FcCHO; (E) CMC of FcCOS determined by surface tension on a TFE platform.

the particles was determined by DLS. As shown in Fig. 2a and b, the irregular sphere micelles at 1 mg/mL were approximately 151 nm and the size distribution was relatively narrow. The self-assembly morphology changes with increasing solution concentration. Vesicles appeared when the concentration reached 10 mg/mL, and the average particle size was approximately 271 nm (Fig. 2c and d). When the concentration was increased further to 20 mg/mL, the vesicles became bigger and the size distribution showed two peaks at approximately 656 and 101 nm by DLS (Fig. 2e and f). As shown in Scheme 1, when dispersed in an acidic solution, FcCOS nanoparticles aggregated because of hydrophobic interaction and formed an internal core. Furthermore, the amino groups of COS on the main chain were protonated to ammonium cations and thus repelled each other, resulting in charge accumulation in the outer layer of the particles and causing enhanced dispersion of nanoparticles in water. With the increasing concentration of FcCOS, the large amount of Fc aggregated into a layer because of hydrophobic interactions and eventually formed vesicles. However, when the concentration was further increased, the vesicles became bigger and the size distribution showed broad variation and poor uniformity.

3.3. Responsive behavior of pH change and oxidative stimulation

Response of FcCOS nanoparticles triggered by pH change (ranging from pH 3.9 to pH 7.1) was investigated by UV–vis spectrophotometry. As shown in Fig. 3A, the nanoparticles were homodispersed in weak acid aqueous solution with a characteristic absorption peak at 474 nm. The nanoparticles were spherical and dispersed uniformly (Fig. 3B). As pH increased, the solubility of COS decreased and the solution became turbid. When the pH value reached 7.1, flocculent precipitate appeared and aggregated at the bottom after a few minutes. Protons in the solution bonded with amino groups to form ammonium ions, and the solubility of the polymer increased. With the increase in pH, the amount of ammonium ions attached to the surface of nanoparticles decreased, which led to the decreased solubility of nanoparticles and appearance of flocculent precipitate (Fig. 3C). The characteristic absorption peaks exhibits a blue shift because the Fc group was altered by protons. The results show that FcCOS nanoparticles have a good response to various pH conditions.

NaClO is an important oxidizing agent in biological experiments (Schuck, De Luca, Peralba, & De Luca, 2006). After NaClO was added,

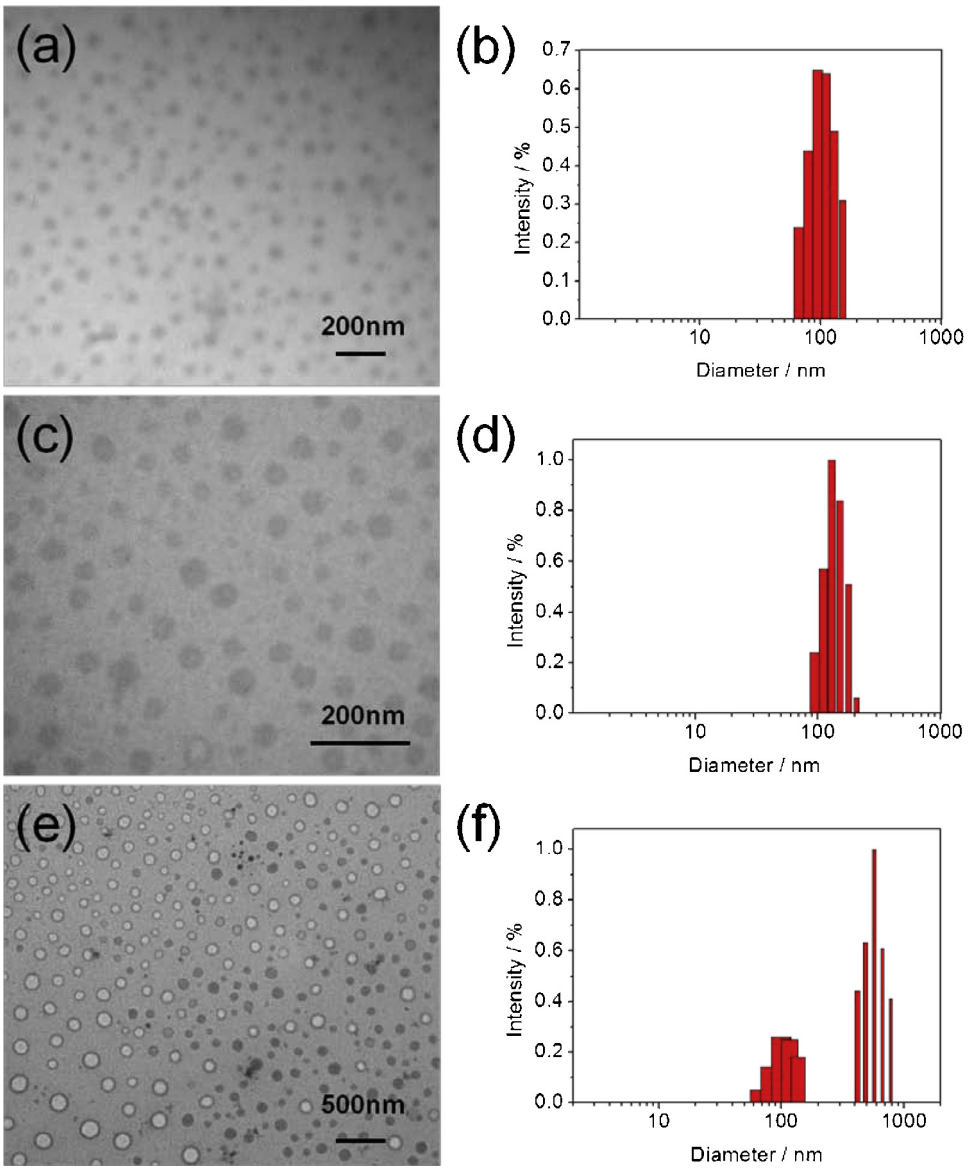

Fig. 2. TEM and particle size distribution histograms by DLS of FcCOS nanoparticles at different concentration: (a, b) 1 mg/mL; (c, d) 10 mg/mL; (e, f) 20 mg/mL.

a characteristic peak at 462 nm that was attributed to the Fc group (in reduced form) became weaker (Fig. 4a). A new characteristic peak of ferrocenium appeared at 632 nm, which indicated that the Fc group was oxidized by NaClO. However, as the concentration was increased up to 0.9%, flocculent precipitate appeared in the mixed solution. On one hand, the nanoparticles were disassembled by HClO hydrolyzed from NaClO. On the other hand, NaOH, another resultant hydrolyzed from NaClO, consumed the protons, causing the pH value to increase. The protons in the solution bonded with amino groups were reduced and dispersion of the assembly was decreased.

To study the oxidation response of FcCOS nanoparticles, low concentrations of H_2O_2 were used as trigger and added into the system. After H_2O_2 addition, the original FcCOS nanoparticle solutions faded. As shown in Fig. 4b, the characteristic absorption peak at 465 nm became weaker when H_2O_2 concentration increased. As the concentration reached 0.9%, the characteristic absorption peak became less noticeable. The result may be caused by two processes: the oxidation of Fc and the degradation of COS based on the reaction of ferrous ion and H_2O_2. Fenton reaction produces hydroxyl free radicals and facilitates COS degradation (Chang, Tai, & Cheng, 2001; Kocha, Yamaguchi, Ohtaki, Fukuda, & Aoyagi, 1997). FcCOS molecules that were broken down to smaller molecules showed better solubility in water. FcCOS nanoparticles can also be triggered through air oxidation. Fc can be easily oxidized by oxygen under acidic condition (Zotti, Schiavon, Zecchin, Berlin, & Pagani, 1998). Therefore, in our experiment, oxygen dissolved in the acid solution was used to trigger disassembly. From Fig. 4c, we observed that the absorbance of the Fc group at 472 nm is unrecognizable after approximately 2 h, indicating that the content of Fc decreases sharply. Ferrocene is known to be very stable in oxygen without acids, because its redox potential ($E^0_{Cp_2Fe^+/Cp_2Fe}$ = 0.59 V) is higher than that of oxygen ($E^0_{O_2^-/O_2}$ = −0.56 V), whereas the oxidative power of oxygen increases considerably in the presence of acids. Fomin (2007) believed that the reaction with oxygen involves the protonated Fc molecule that acts as a donor of atomic hydrogen, which is favored by the low energy of the Fe–H bond. To confirm the oxidation mechanism in acid solution, FcCOS was dissolved in a pH 3.8 buffer and investigated by CV (Fig. 4d). The nanoparticles of FcCOS exhibited an initial oxidation behavior at approximately 0.414 V and a secondary oxidation peak at 0.567 V,

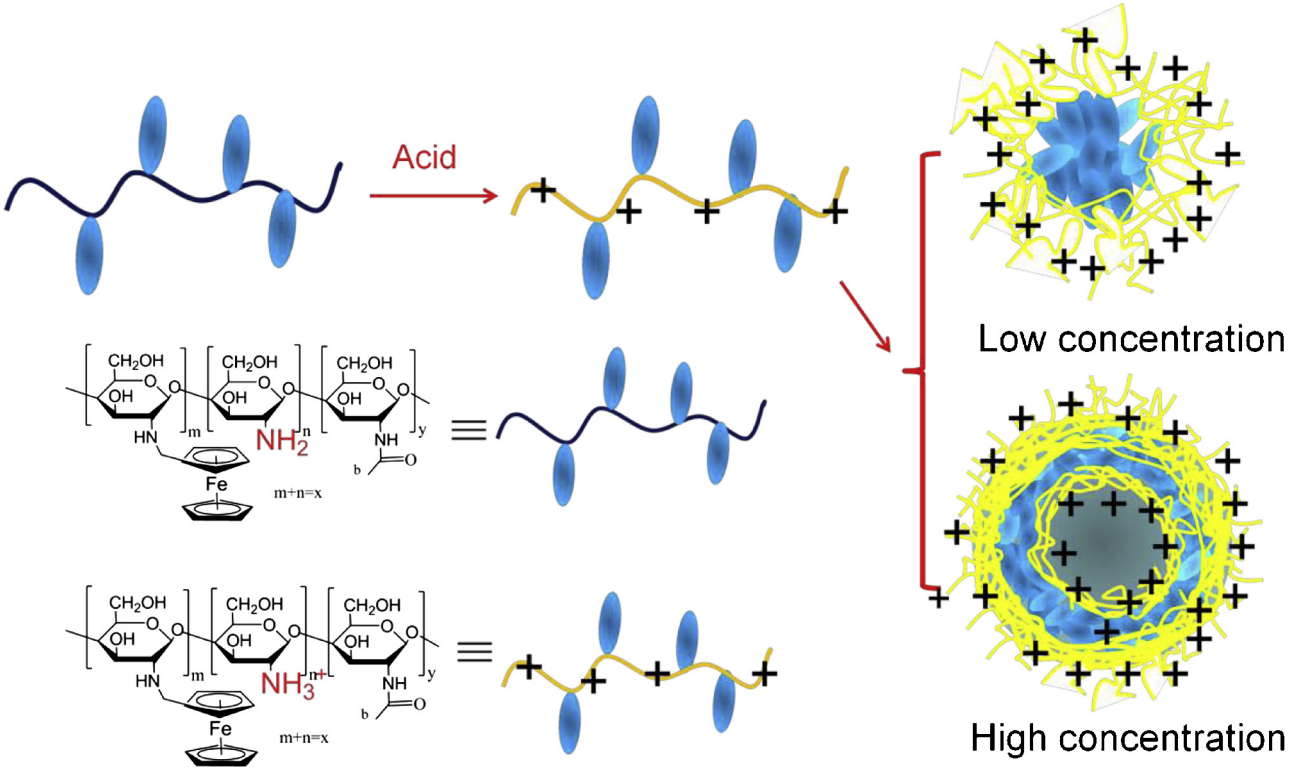

Scheme 1. Illustration of self-assembly behavior of FcCOS nanoparticles at different concentrations.

which is attributed to Cp_2Fe/Cp_2Fe^+. In addition, the new oxidation peak at approximately 0.271 V can be attributed to a site-specific fragmentation of the β-1 and 4 glycosidic linkages. The characterization results suggested that the occurrence of the oxidation of FcCOS molecules.

3.4. Loading and in vitro release of 5-FU

The size of drug-loaded particles may affect the ability of a system to deliver drugs effectively for practical application. If the size of the particles exceeds 300 nm, then most of the particles would be captured by filtration in the red pulp of the spleen and phagocytosed within the cells of the reticuloendothelial system (Yang & Hon, 2009). In our experiment, 5-FU and FcCOS were mixed to form a homogeneous disperse mixture based on emulsion–solvent evaporation (Chung, Huang, & Liu, 2001; Qiu, Wang, Zheng, Jin, & Jin, 2010). The concentration of FcCOS was approximately 1 mg/mL. The obtained 5-FU/FcCOS nanoparticles were observed by TEM. As shown in Fig. 5a, 5-FU/FcCOS nanospheres had a uniform geometrical shape with an average size of approximately 238 nm, as characterized by DLS (Fig. 5b). The loading capacity and encapsulation efficiency were 9.67% and 56.80%, respectively, as determined by UV–vis spectrophotometry.

The in vitro release of 5-FU from FcCOS nanoparticles was investigated at 37 °C under different pH conditions [(i) pH 7.4, (ii) pH 6.8, and (iii) pH 3.8]. To investigate pH effects independently, nitrogen

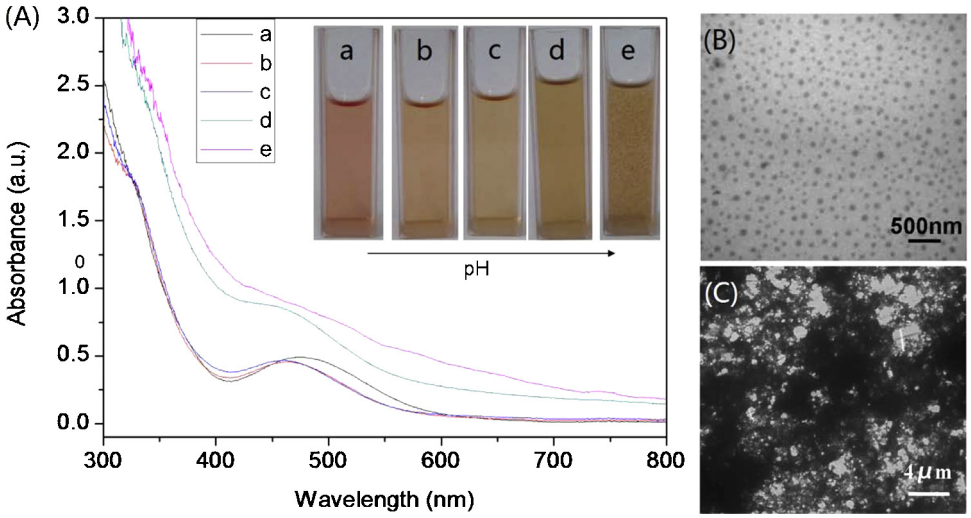

Fig. 3. (A) pH responses of FcCOS nanoparticles: a, pH 3.9; b, pH 4.5; c, pH 5.1; d, pH 6.7; e, pH 7.1; (B) TEM of FcCOS nanoparticles at pH 3.9; (C) TEM of FcCOS flocculated precipitate at pH 7.1.

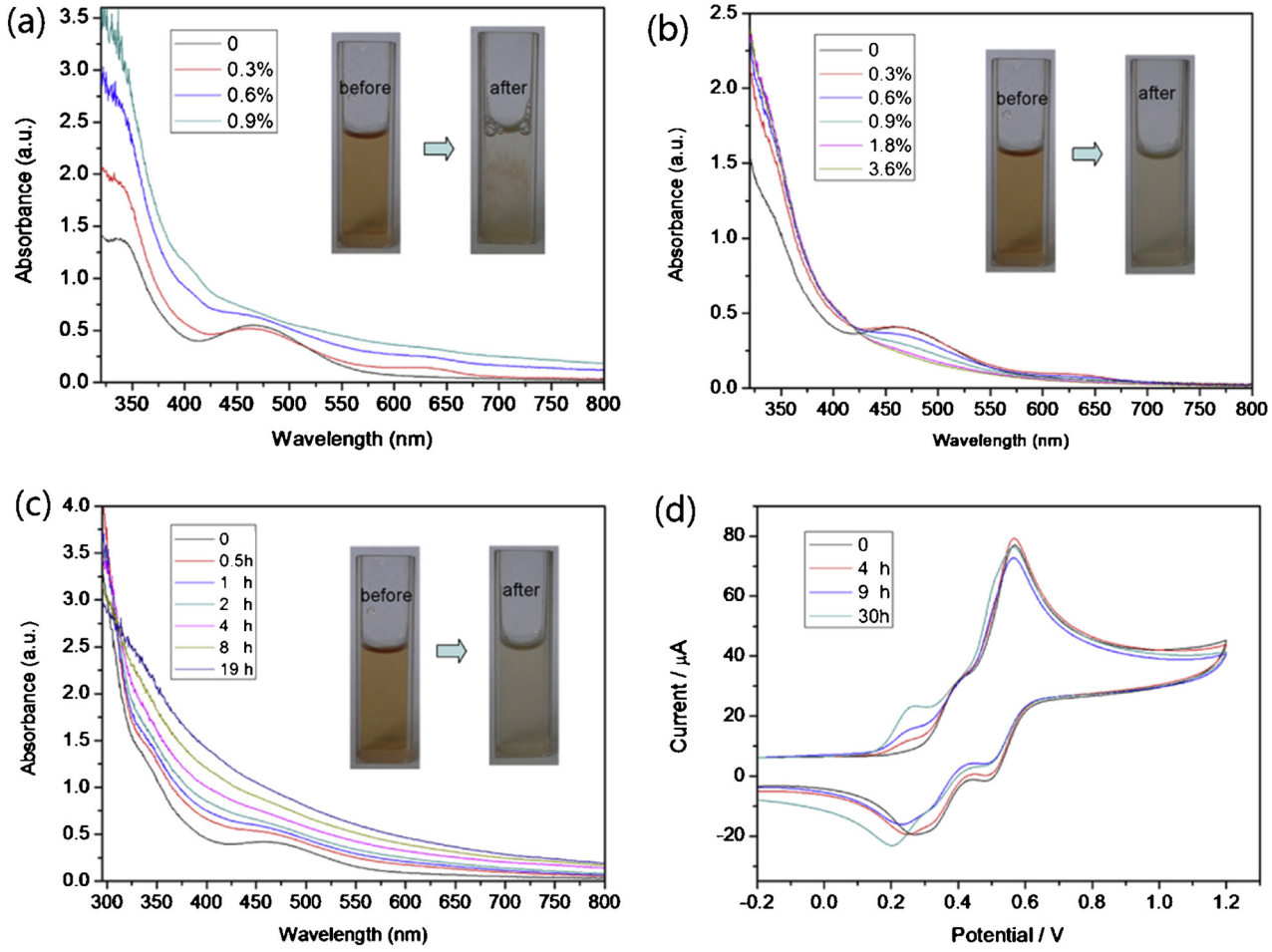

Fig. 4. Oxidation responses of FcCOS nanoparticles: (a) UV–vis spectrogram of solution added NaClO; (b) UV–vis spectrogram of solution added H_2O_2; (c) UV–vis spectrogram of solution bubbled air; (d) CV of solution exposed in air.

(N_2) was bubbled into all buffers for 0.5 h in advance. As shown in Fig. 6, the accumulative release increased from 29.15% to 49.02% with the decrease of pH. Given the increased number of protons in the system, the cationic nanoparticles swelled, reduced the binding of drug molecules, and released the unbounded drugs into the system. However, a sudden release occurred because of the dispersion of nanoparticles by ultrasound in buffers. An initial burst at pH 3.8 and 6.8 is attributed to the rapid dissociation of hydrogen bonds between 5-FU molecules and $-NH_2$ of COS.

The accumulative in vitro release curve was also investigated with air bubbled into buffers at pH 3.8. In Fig. 6, the sample with bubbled air has a higher accumulative release up to 59.64%, compared with samples with bubbled N_2 just up to 49.02%. Scheme 2 shows the drug-releasing behavior of FcCOS nanoparticles in the presence of oxidative agent at different pH conditions. Protonated ammonium cations have target identification to negatively charged receptors (Davis, 2008). After the nanoparticles were swallowed, the ammonium cations would swell and peel off layer by layer because of electrostatic repulsion. When Fc was oxidated to ferrocenium by oxygen, π–π stacking effect disappeared immediately. Under the synergistic effect of oxidative agent and low pH, FcCOS nanoparticles disassembled faster and the release of drug

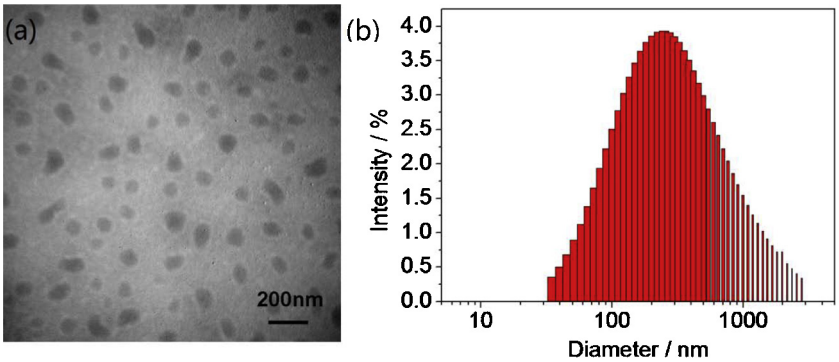

Fig. 5. TEM and DLS histograms of FcCOS nanoparticles 1 mg/mL: (a) TEM of FcCOS nanoparticles loading 5-FU 1 mg/mL; (b) DLS determined size distribution which mean particle size were 238 nm.

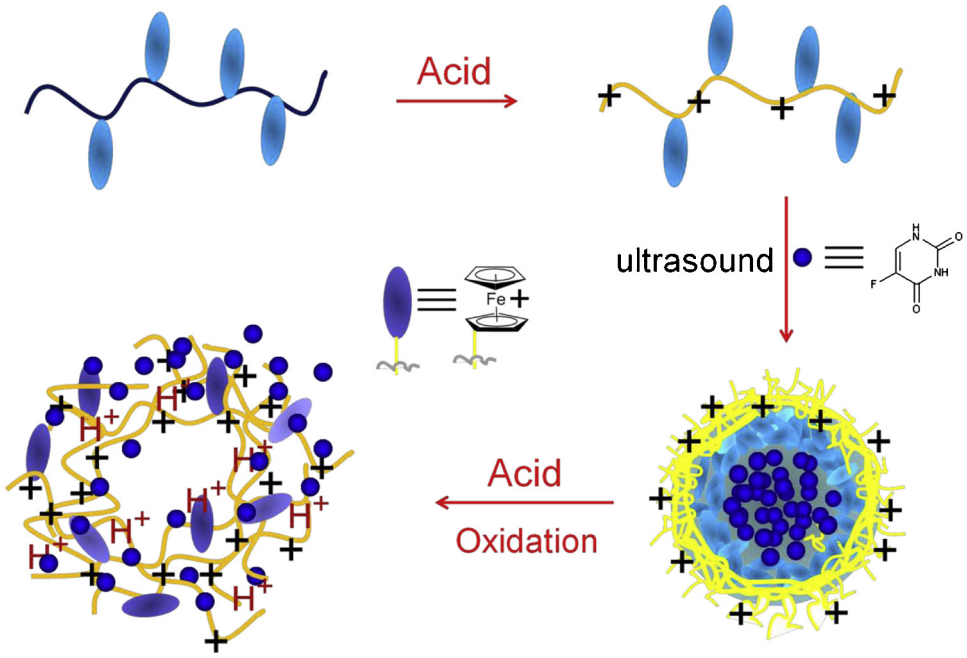

Scheme 2. Illustration of drug-releasing behavior of FcCOS nanoparticles in the presence of oxidative agent at different pH conditions.

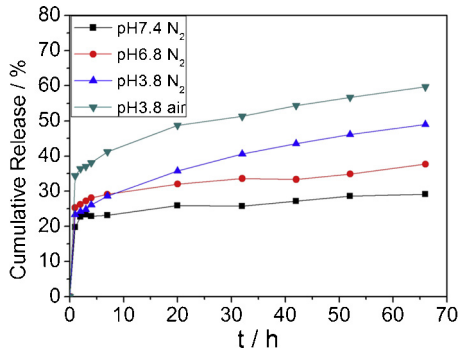

Fig. 6. pH and oxidation responsive 5-FU release profiles of the 5-FU loaded micelles in the release media: (i) pH 7.4 N_2, (ii) pH 6.8 N_2, (iii) pH 3.8 N_2, (iv) pH 3.8 air.

molecules was accelerated. In addition, FcCOS nanoparticles itself can exhibit anti-cancer properties and are biodegradable and biocompatible. Thus, FcCOS nanoparticles have high potential in drug delivery.

4. Conclusions

In this study, nanoparticles based on Fc-modified COS were constructed via hydrophobic effect of Fc self-assembly in aqueous solution. The nanoparticles are responsive to pH change, particularly to weak acid. NaClO, H_2O_2 and oxygen accelerate the disassembly progress. Meanwhile, 5-FU, as a drug model, was integrated efficiently with an encapsulation efficiency of up to 56.80%. The accumulative release rate of the sample under aerobic condition reached up to 59.64% at pH 3.8 while it is just 49.02% under bubbled N_2 at the same pH value, which showed a significant synergistic effect between oxidative and pH responses. Therefore, the FcCOS nanoparticles can be developed as potential pH and oxidation dual-responsive carriers to enhance drug efficacy for cancer treatment.

Acknowledgement

This research was supported by the Foundation of University of Chinese Academy of Sciences (Y25102CN00 and Y0JT017J01).

References

Angelatos, A. S., Radt, B., & Caruso, F. (2005). Light-responsive polyelectrolyte/gold nanoparticle microcapsules. *The Journal of Physical Chemistry B*, *109*(7), 3071–3076.

Aydin, R., & Pulat, M. (2012). 5-Fluorouracil encapsulated chitosan nanoparticles for pH-stimulated drug delivery: Evaluation of controlled release kinetics. *Journal of Nanomaterials*, *42*, 1–10.

Borrelli, A., Schiattarella, A., Bonelli, P., Tuccillo, F. M., Buonaguro, F. M., & Mancini, A. (2014). The functional role of MnSOD as a biomarker of human diseases and therapeutic potential of a new isoform of a human recombinant MnSOD. *BioMed Research International*, *2014*, 476789.

Chang, K. L. B., Tai, M.-C., & Cheng, F.-H. (2001). Kinetics and products of the degradation of chitosan by hydrogen peroxide. *Journal of Agricultural and Food Chemistry*, *49*(10), 4845–4851.

Chen, Y., Chen, Y., Xiao, D., Bose, A., Deng, R., & Bothun, G. D. (2014). Low-dose chemotherapy of hepatocellular carcinoma through triggered-release from bilayer-decorated magnetoliposomes. *Colloids and Surfaces B: Biointerfaces*, *116*(4), 452–458.

Cheng, R., Meng, F., Deng, C., Klok, H.-A., & Zhong, Z. (2013). Dual and multi-stimuli responsive polymeric nanoparticles for programmed site-specific drug delivery. *Biomaterials*, *34*(14), 3647–3657.

Chung, T. W., Huang, Y. Y., & Liu, Y. Z. (2001). Effects of the rate of solvent evaporation on the characteristics of drug loaded PLLA and PDLLA microspheres. *International Journal of Pharmaceutics*, *212*(2), 161–169.

Clark, G. L., & Smith, A. F. (1936). X-ray diffraction studies of chitin, chitosan, and derivatives. *The Journal of Physical Chemistry*, *40*(7), 863–879.

Davis, M. E. (2008). Nanoparticle therapeutics: An emerging treatment modality for cancer. *Nature Reviews Drug Discovery*, *7*(9), 771–782.

Duan, Q., Cao, Y., Li, Y., Hu, X., Xiao, T., Lin, C., et al. (2013). pH-responsive supramolecular vesicles based on water-soluble pillar [6] arene and ferrocene derivative for drug delivery. *Journal of the American Chemical Society*, *135*(28), 10542–10549.

Fomin, V. (2007). Common relationships of ferrocene oxidation with oxygen and sulfur dioxide in acid solutions and of its direct oxidation with carboxylic acids. *Russian Journal of General Chemistry*, *77*(5), 954–960.

Fouda, M. F. R., Abd-Elzaher, M. M., Abdelsamaia, R. A., & Labib, A. A. (2007). On the medicinal chemistry of ferrocene. *Applied Organometallic Chemistry*, *21*(8), 613–625.

Garcia, A., Peniche-Covas, C., Chico, B., Simpson, B. K., & Villalonga, R. (2007). Ferrocene branched chitosan for the construction of a reagentless amperometric hydrogen peroxide biosensor. *Macromolecular Bioscience*, *7*(4), 435–439.

Ge, Z., & Liu, S. (2013). Functional block copolymer assemblies responsive to tumor and intracellular microenvironments for site-specific drug delivery and enhanced imaging performance. *Chemical Society Reviews*, *42*(17), 7289–7325.

Hirai, A., Odani, H., & Nakajima, A. (1991). Determination of degree of deacetylation of chitosan by ^{1}H NMR spectroscopy. *Polymer Bulletin*, *26*(1), 87–94.
Kim, S.-K., & Rajapakse, N. (2005). Enzymatic production and biological activities of chitosan oligosaccharides (COS): A review. *Carbohydrate Polymers*, *62*(4), 357–368.
Kimura, Y., & Okuda, H. (1999). Prevention by chitosan of myelotoxicity, gastrointestinal toxicity and immunocompetent organic toxicity induced by 5-fluorouracil without loss of antitumor activity in mice. *Cancer Science*, *90*(7), 765–774.
Kocha, T., Yamaguchi, M., Ohtaki, H., Fukuda, T., & Aoyagi, T. (1997). Hydrogen peroxide-mediated degradation of protein: Different oxidation modes of copper-and iron-dependent hydroxyl radicals on the degradation of albumin. *Biochimica et Biophysica Acta (BBA)-Protein Structure and Molecular Enzymology*, *1337*(2), 319–326.
Kumar, S., & De, P. (2014). Fluorescent labelled dual-stimuli (pH/thermo) responsive self-assembled side-chain amino acid based polymers. *Polymer*, *55*(3), 824–832.
Li, M.-H., & Keller, P. (2009). Stimuli-responsive polymer vesicles. *Soft Matter*, *5*(5), 927–937.
Liu, M., Deng, J., Chen, Q., Huang, Y., Wang, L., Zhao, Y., et al. (2012). Sensitive detection of rutin with novel ferrocene benzyne derivative modified electrodes. *Biosensors and Bioelectronics*, *41*, 275–281.
Motornov, M., Roiter, Y., Tokarev, I., & Minko, S. (2010). Stimuli-responsive nanoparticles, nanogels and capsules for integrated multifunctional intelligent systems. *Progress in Polymer Science*, *35*(1), 174–211.
Qiu, L. Y., Wang, R. J., Zheng, C., Jin, Y., & Jin, L. Q. (2010). β-Cyclodextrin-centered star-shaped amphiphilic polymers for doxorubicin delivery. *Nanomedicine*, *5*(2), 193–208.
Rejinold, N. S., Muthunarayanan, M., Chennazhi, K., Nair, S., & Jayakumar, R. (2011). 5-Fluorouracil loaded fibrinogen nanoparticles for cancer drug delivery applications. *International Journal of Biological Macromolecules*, *48*(1), 98–105.
Salonen, J., Laitinen, L., Kaukonen, A. M., Tuura, J., Bjorkqvist, M., Heikkila, T., et al. (2005). Mesoporous silicon microparticles for oral drug delivery: Loading and release of five model drugs. *Journal of Controlled Release: Official Journal of the Controlled Release Society*, *108*(2–3), 362–374.
Schuck, C. A., De Luca, S. J., Peralba, M. D. C. R., & De Luca, M. A. (2006). Sodium ferrate (IV) and sodium hypochlorite in disinfection of biologically treated effluents. Ammonium nitrogen protection against THMs and HAAs. *Journal of Environmental Science and Health Part A*, *41*(10), 2329–2343.
Shi, J., Alves, N. M., & Mano, J. F. (2008). Chitosan coated alginate beads containing poly (N-isopropylacrylamide) for dual-stimuli-responsive drug release. *Journal of Biomedical Materials Research Part B: Applied Biomaterials*, *84*(2), 595–603.
Song, C.-C., Ji, R., Du, F.-S., & Li, Z.-C. (2013). Oxidation-responsive poly(amino ester)s containing arylboronic ester and self-immolative motif: Synthesis and degradation study. *Macromolecules*, *46*(21), 8416–8425.
Sun, X., Shi, J., Xu, X., & Cao, S. (2013). Chitosan coated alginate/poly (N-isopropylacrylamide) beads for dual responsive drug delivery. *International Journal of Biological Macromolecules*, *59*, 273–281.
Top, S., Vessieres, A., Cabestaing, C., Laios, I., Leclercq, G., Provot, C., et al. (2001). Studies on organometallic selective estrogen receptor modulators. (SERMs) Dual activity in the hydroxy-ferrocifen series. *Journal of Organometallic Chemistry*, *637*, 500–506.
Wang, L., Li, Y.-K., Xu, Y., & Wang, C.-Q. (2014). A facile construction method for pH and oxidation dual-responsive assembly based on ferrocene-modified chitooligosaccharide. *Reactive and Functional Polymers*, *76*, 1–7.
Wang, Y., Chen, L., Ding, Y., & Yan, W. (2012). Oxidized phospholipid based pH sensitive micelles for delivery of anthracyclines to resistant leukemia cells in vitro. *International Journal of Pharmaceutics*, *422*(1–2), 409–417.
Wei, Q. B., Luo, Y. L., Fu, F., Zhang, Y. Q., & Ma, R. X. (2012). Synthesis, characterization, and swelling kinetics of pH-responsive and temperature-responsive carboxymethyl chitosan/polyacrylamide hydrogels. *Journal of Applied Polymer Science*, *129*(2), 806–814.
Wen, L., Li, M., & Wu, Y. (2012). Monodisperse pH-sensitive protamine hollow microspheres as carriers for drug delivery. *Journal of Applied Polymer Science*, *129*(2), 568–576.
Weschayanwiwat, P., Scamehorn, J. F., & Reilly, P. J. (2005). Surfactant properties of low molecular weight phospholipids. *Journal of Surfactants and Detergents*, *8*(1), 65–72.
Xia, W., Liu, P., Zhang, J., & Chen, J. (2011). Biological activities of chitosan and chitooligosaccharides. *Food Hydrocolloids*, *25*(2), 170–179.
Xuan, J., Han, D., Xia, H., & Zhao, Y. (2014). Dual-stimuli-responsive micelle of an ABC triblock copolymer bearing a redox-cleavable unit and a photocleavable unit at two block junctions. *Langmuir*, *30*(1), 410–417.
Yang, H.-C., & Hon, M.-H. (2009). The effect of the molecular weight of chitosan nanoparticles and its application on drug delivery. *Microchemical Journal*, *92*(1), 87–91.
Zhou, S., Du, X., Cui, F., & Zhang, X. (2013). Multi-responsive and logic controlled release of DNA-gated mesoporous silica vehicles functionalized with intercalators for multiple delivery. *Small*, *10*(5), 980–988.
Zhu, L., Shangguan, Y., Sun, Y., Ji, J., & Zheng, Q. (2010). Rheological properties of redox-responsive, associative ferrocene-modified branched poly (ethylene imine) and its modulation by β-cyclodextrin and hydrogen peroxide. *Soft Matter*, *6*(21), 5541–5546.
Zotti, G., Schiavon, G., Zecchin, S., Berlin, A., & Pagani, G. (1998). Adsorption of ferrocene compounds on indium-tin-oxide electrodes. Enhancement of adsorption by decomposition of ferrocenium molecules by oxygen. *Langmuir*, *14*(7), 1728–1733.